EMITTANCE GROWTH INDUCED BY MICROBUNCHING INSTABILITY IN THE FERMI@ELETTRA HIGH ENERGY TRANSFER LINE

S. Di Mitri[#], W. Barletta, M. Cornacchia, Sincrotrone Trieste (ELETTRA), Trieste, Italy

Abstract

   Simulations of the microbunching instability through the FERMI@elettra lattice have been carried out with *elegant* particle tracking code. This paper focuses on the emittance growth induced by the microbunching instability in the high energy transfer line that guides the electron beam from the linac to the undulator chain. The perturbation to the transverse emittance induced by coherent synchrotron radiation and longitudinal space charge as function of the R_{56} transport matrix element in the transfer line have been investigated separately and in the presence of their mutual interaction. Simulation results show that the betatron phase mismatch may have a detrimental impact on the final beam emittance.

INTRODUCTION

   Simulations of the microbunching instability [1] through the FERMI@elettra lattice [2] have been carried out with LiTrack [3] and *elegant* [4] particle tracking codes. This note focuses on the projected emittance growth induced by the microbunching instability in the Spreader, the high energy dog-leg that guides the electron beam from the linac to the undulator chain.

   The instability development is simulated from the injector end (97 MeV) to the Spreader end (1.5 GeV). It is driven in the accelerator by Longitudinal Space Charge (LSC) [5], Coherent Synchrotron Radiation (CSR) [6] and energy dispersion. CSR induced energy loss establishes a correlation with the longitudinal coordinate along the bunch. Since this happens in a dispersive region (in the magnetic chicane of the bunch compressor and in the achromat region of the Spreader), different longitudinal slices of the bunch start their betatron oscillations around different trajectories. Hence, while the slice transverse emittance is not generally affected by CSR, the projected emittance is. It is also clear that the CSR emittance growth is even more degraded by the presence of LSC because it amplifies the CSR emission [1].

   Simulations have been carried out for the FEL1 Spreader branch (called SFEL1) [2]. It consists of two identical achromats, each of two 3 deg bending magnets separated by four quadrupoles. The quadrupoles are used to: i) match the dispersion function in the achromat; ii) make the line isochronicity and achromaticity adjustable by the user; iii) make the betatron phase advance between two consecutive dipoles equal to π (-*I* transport matrix). In this way, the CSR transverse kick in a dipole is compensated by the kick in the succeeding one, and the projected emittance growth is cancelled [7].

   Figure 1 shows the optics functions from the injector end to the SFEL1 end for matched (R_{56}=0mm) and

mismatched (R_{56}= -6mm) dispersion in the Spreader. The optics mismatch is caused by a 10% gradient error of quadrupoles in the achromats; the error is randomly distributed over the four quadrupoles of each achromat. We anticipate that the betatron phase mismatch, which is the corruption of the –*I* transport matrix, may have a detrimental impact on the final beam emittance.
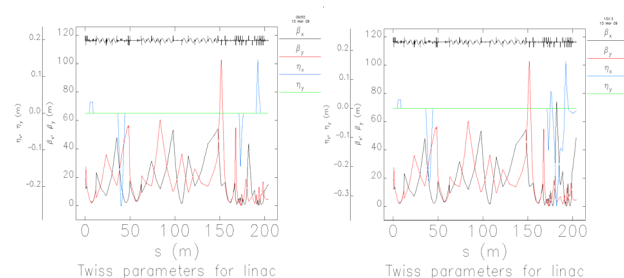

Figure 1: FERMI@elettra optics functions from the injector end to the SFEL1 branch line end. Horizontal dispersion in the Spreader is matched for R_{56}=0mm (left) and mismatched for R_{56}= -6mm (right).

SMOOTHING AND REPOPULATION

   The smoothing and repopulating algorithm called smoothDist6D, provided by M. Borland (ANL), is implemented to avoid unphysical tracking results due to numerical sampling noise anomalies.

   To get rid of possible changes in the original particle distribution by the algorithm, the particle file was checked before and after the manipulation, at the beginning of acceleration (97 MeV).

   Figure 2 depicts the initial longitudinal particle distribution for the original and smoothed particle file. Figure 3 shows contour plots of the initial transverse phase space, where the color code refers to the "action" of a particle, i.e. the square root of its Courant-Snyder invariant (or "emittance"), in increasing order from red to violet. Figure 4 shows the computed projected emittance as function of the number of particles in the transverse phase space.

   All these preliminary studies demonstrate that the smoothing and repopulating process does its job of preserving the macroscopic structure of the beam both in the longitudinal and in the transverse plane. However, a small change in the transverse particle distribution can be observed in Figure 4. Here, although the 100% emittance has the same value before and after the file manipulation, it assumes a slightly different value as for the 90% of particles ($0.75 \cdot 10^{-6}$ m rad before, $0.8 \cdot 10^{-6}$ m rad after the file manipulation).
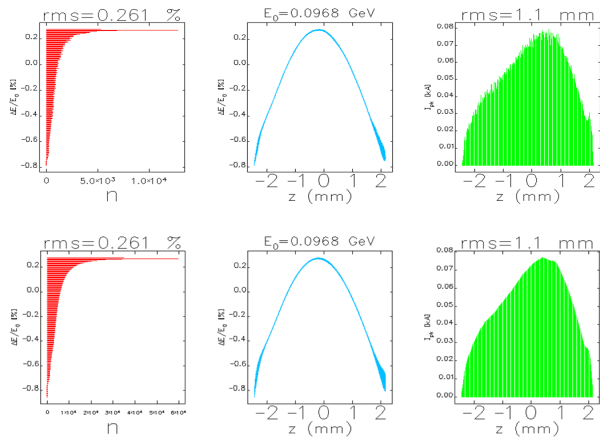

[#]simone.dimitri@elettra.trieste.it

Figure 2: Initial particle distribution. From left to right: energy distribution, longitudinal phase space, current profile. Top line is for $2 \cdot 10^5$ particles from GPT code [8]. Bottom line is for 10^6 particles repopulated and smoothed.
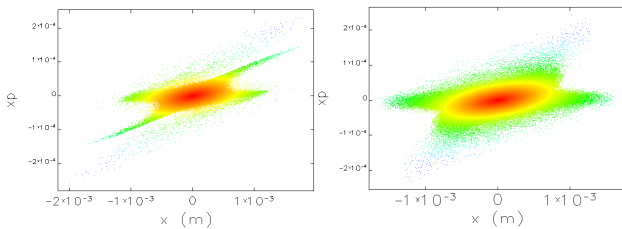

Figure 3: Horizontal phase space for $2 \cdot 10^5$ (left) and 10^6 particles (right) at the injector end (97MeV). Colour scale from red to violet is proportional to the particle horizontal invariant.
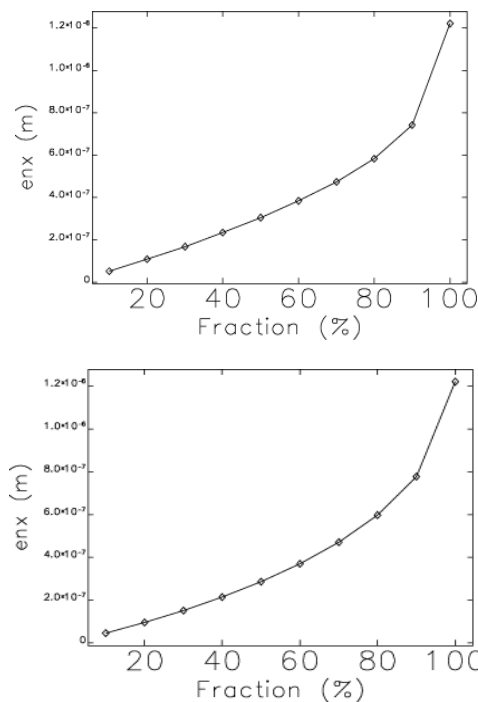

Figure 4: Normalised horizontal projected emittance as function of the percentage of particles in the transverse phase space at 97MeV, for $2 \cdot 10^5$ (left) and 10^6 (right) particles.

PROJECTED EMITTANCE GROWTH

CSR Instability

The rms projected emittance behavior has been investigated with tracking of $2 \cdot 10^5$ particles in *elegant*, for the matched (R_{56}=0mm) and mismatched (R_{56}= -6mm) configuration of the Spreader lattice; as of yet, no LSC is considered. In the former case, the projected emittance is preserved in the Spreader at the value of $1.4 \cdot 10^{-6}$ m rad, which is obtained at the entrance of the transfer line; the emittance grows to $1.55 \cdot 10^{-6}$ m rad in the latter case.

Since no difference between these results and those for 10^6 particles has been observed, we deduce that: i) the smoothing and repopulating algorithm preserves the longitudinal and transverse particle distribution; ii) the simulation of the CSR instability is not sensitive to the present level of numerical noise.

LSC Instability

Same simulations as in the previous Section were repeated with $2 \cdot 10^5$ particles by including LSC in the whole linac. While the matched optics still preserves the rms projected emittance at the $1.4 \cdot 10^{-6}$ m rad baseline, the unmatched one allows emittance to grow up to $1.7 \cdot 10^{-6}$ m rad.

The mismatched case was repeated with 10^6 particles; it provides a slightly different result than with $2 \cdot 10^5$ particles, that is a final – smaller – rms projected emittance of $1.55 \cdot 10^{-6}$ m rad. Indeed, the fractional emittance distribution at the end of the transfer line has changed as the number of particle in the simulation has increased, as shown in Figure 5.
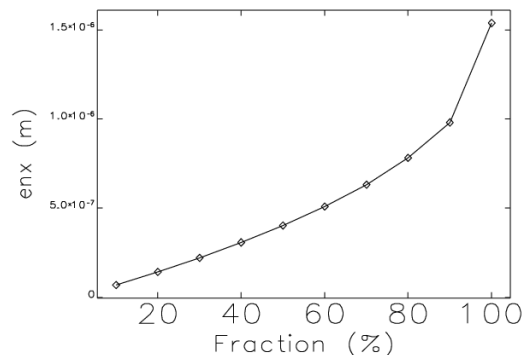

Figure 5: Same as in Figure 4, but now 10^6 particles are simulated. To be compared with Figure 4, bottom plot.

In order to confirm the effect of the numerical noise on the simulation result when the LSC is present, we also report the particle longitudinal distribution in Figure 6. The longitudinal phase space is clearly different in the case of $2 \cdot 10^5$ and 10^6 particles. In the latter scenario, a few particles in the bunch head have a bigger energy spread (up to 3%); the current modulation in the bunch core is reduced in amplitude, while the edge spikes are two times higher than in the $2 \cdot 10^5$ particle case.

Now, if we compare the results in this Section with those in the previous one, we can infer that the presence of LSC makes the *elegant* simulation of the microunching instability more sensitive to the numerical sampling noise. In particular, the fact that the final projected emittance becomes smaller when increasing the number of particles, leads to the conclusion that the real projected emittance growth induced by optics mismatch is over-estimated by the present simulations.
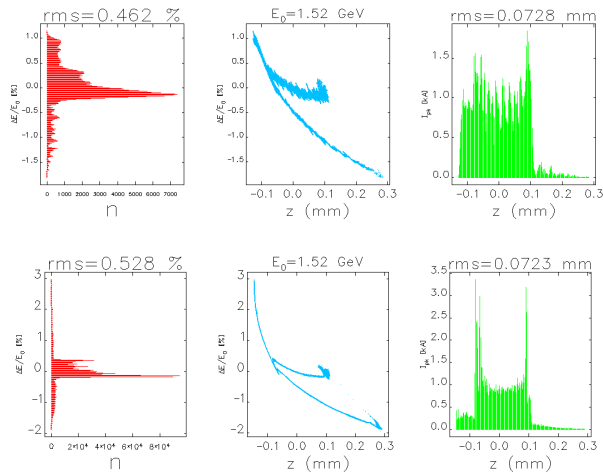

Figure 6: Final particle distribution from 1-D tracking in Litrack code [8]. From left to right: energy distribution, longitudinal phase space, current profile. Top line is for $2 \cdot 10^5$ particles from. Bottom line is for 10^6 particles repopulated and smoothed.

CONCLUSIONS

The impact of the microbunching instability on the horizontal projected emittance in the FERMI FEL1 Spreader branch line was studied with *elegant* and LiTrack particle tracking code. The Spreader lattice was simulated with matched and mismatched betatron phase advance, respectively. In the nominal matched case, microbunching compensates the CSR induced emittance growth.

The simulations were carried out with a number of particles insufficient to control the numerical sampling noise, which is intrinsic in the codes. Therefore, as the instability becomes stronger, the final transverse and longitudinal particle distribution is dependent on the number of particles in the simulation.

More in detail, if CSR only is present (weak instability due to reduced gain, see also [9]) this study verifies that the final particle distribution does not depend on the smoothing and repopulating process of the initial beam. In contrast, LSC makes the instability much stronger [5]. In this case, if the optics remains matched, there is no emittance degradation. But, when the optics is mismatched, the effect of numerical noise becomes visible and the final degraded emittance becomes smaller as the number of particles is increased.

In general, the results listed in Table 1 are considered pessimistic because the simulations are affected by the

numerical noise, therefore they over-estimate the real effect. Moreover, no beam heating [1,2] was included in the simulations to damp the instability. Thus, an error even as large as 10% in the Spreader quadrupole gradients is not a big issue for the preservation of the horizontal projected emittance.

Table 1: Absolute increment of the normalised horizontal projected emittance (rms value in mm mrad) *without* chromatic contribution to the beam size. The first number in each column refers to simulation with $2 \cdot 10^5$ particles, the second one to simulation with 10^6 particles. The emittance value for the bare lattice is 1.4 mm mrad.

Configuration	$R_{56} = 0$mm	$R_{56} = -6$mm
Bare lattice	≤ 0.01	≤ 0.01
CSR only	$< 0.05, < 0.05$	0.15, 0.15
CSR + LSC	$< 0.05, < 0.05$	0.3, 0.15

REFERENCES

[1] E. Saldin, E. Schneidmiller, M. Yurkov, NIM A, **490**, (2002), 1.
[2] S. Di Mitri et al., NIM A **608** (2009), 19–27.
[3] K. Bane P. Emma, PAC'05, Knoxville, Tennessee, USA (2005).
[4] M. Borland, APS LS–287 (2000).
[5] E. L. Saldin, E. A. Schneidmiller, M. V. Yurkov, TESLA_FEL-2003-02 (2003).
[6] Y. Derbenev, J. Rossbach, E. Saldin, V. Shiltsev, TESLA-FEL 95-05 (1995).
[7] D. Douglas, JLAB-TN-98-012 (1998).
[8] S. B. van der Geer, M. J. de Loos, http://www.pulsar.nl/gpt.
[9] M. Venturini, et al., PRST-AB, **10** (2007) 104401.